THE JOURNAL OF PHYSICAL CHEMISTRY C

ARTICLE

pubs.acs.org/JPCC

Screening of Electrocatalysts for Photoelectrochemical Water Oxidation on W-Doped $BiVO_4$ Photocatalysts by Scanning Electrochemical Microscopy

Heechang Ye, Hyun S. Park, and Allen J. Bard*

Center for Electrochemistry, Department of Chemistry and Biochemistry, The University of Texas at Austin, Austin, Texas 78712, United States

Supporting Information

ABSTRACT: Oxygen evolution reaction (OER) electrocatalyst arrays for photoelectrochemical (PEC) water oxidation were fabricated on a metal oxide semiconductor photoelectrode, W-doped $BiVO_4$ (BiVW-O). The electrocatalysts (IrO_x, Pt, Co_3O_4) were prepared on a drop cast film of BiVW-O on fluorine-doped tin oxide (FTO) with a picoliter solution dispenser or photodeposition with light irradiation through an optical fiber. The prepared arrays were tested for PEC water oxidation in 0.2 M sodium phosphate buffer (pH 6.8) using scanning electrochemical microscopy modified with an optical fiber. Pt and Co oxide electrocatalysts showed an enhanced photocurrent for PEC water oxidation, while the other metal oxide catalysts including IrO_x, which is known as an excellent water oxidation electrocatalyst on a metal substrate, were not effective. These results were confirmed with bulk film studies. A cobalt phosphate (Co-Pi) electrocatalyst was also tested as a bulk film on BiVW-O and showed improvement for PEC water oxidation. Preliminary characterization (X-ray diffraction and X-ray photoelectron spectroscopy) was also performed for these catalysts. The results indicate that considerations of the semiconductor photocatalyst/electrocatalyst interface are important in determining the effectiveness of materials for the photodriven OER.

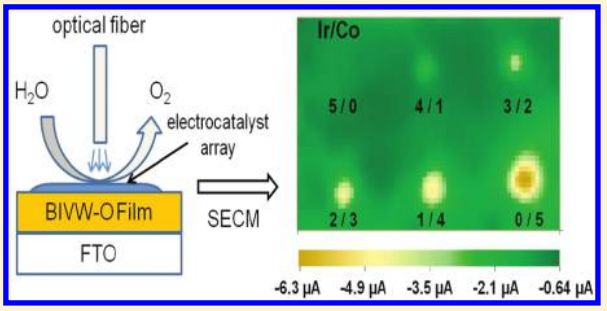

INTRODUCTION

We report a study of various electrocatalysts for photoelectrochemical (PEC) water oxidation on a metal oxide semiconductor electrode by scanning electrochemical microscopy (SECM) with an optical fiber to screen arrays of different materials. Electrocatalysts for the oxygen evolution reaction (OER) are important in water electrolysis, e.g., during production of hydrogen, and have been intensively investigated. These OER electrocatalysts are also of interest for PEC water splitting with semiconductor photocatalysts, where they promote the multielectron OER driven by photon-generated holes. We have previously reported the use of SECM for the rapid screening of electrocatalysts, for example, for oxygen reduction and for the OER.[1,2] An analogous technique can be used, replacing the scanning tip with an optical fiber, to screen semiconductor photocatalysts.[3−6]

PEC water splitting has been proposed as a promising tool to convert solar energy to chemical fuel (hydrogen) since Fujishima and Honda suggested TiO_2 photocatalysis for water splitting under UV light irradiation.[7] Water splitting is composed of two electrochemical half reactions, water oxidation and proton reduction, both of which are heterogeneous inner sphere multielectron reactions. Therefore, electrocatalysts are required to reduce the overpotentials of these reactions. The proton reduction reaction is a two-electron process and can be catalyzed very well by Pt, Pd, and other materials. However, the OER is a more complicated four-electron, four-proton transfer process with oxygen−oxygen bond formation and occurs with significant overpotential even with good electrocatalysts for water oxidation. Many metals and metal oxides, such as IrO_2, RuO_2, Rh_2O_3, Co_3O_4, and Mn oxide, have been investigated as electrocatalysts for photochemical water oxidation as dispersed powders in solution[8−12] or deposited on other powdered photocatalysts in solution.[13−15] In addition, IrO_2,[16−18] RuO_2, Pt (or PtO_2),[19] Ni oxide,[20,21] NiFe oxide,[22−28] Co_3O_4,[25−28] Co phosphate (Co-Pi),[29−31] and Ni borate[32] have been suggested as electrocatalysts for water oxidation in electrochemical systems.[33,34] However, the study of electrocatalysts associated with semiconductor photoelectrodes for PEC water oxidation has been more limited. Grätzel and co-workers reported a Co ion layer[35] and iridium oxide[36] on hematite film showed photocurrent enhancement for water oxidation. Gamelin et al. reported the electrocatalytic activity of Co-Pi water oxidation catalyst on hematite photoelectrodes.[37,38] McFarland et al. also investigated a NiFe oxide electrocatalyst for the PEC water oxidation on Ti-doped hematite photoelectrodes.[39]

Received: January 26, 2011
Revised: May 18, 2011
Published: May 25, 2011

Recently, our group reported a new strategy for fast preparation and screening of photocatalysts for water oxidation using the SECM technique modified by replacing the ultramicroelectrode (UME) tip with an optical fiber[3] and found that a 5% W-doped bismuth vanadate (BiVW-O) showed significantly enhanced photoactivity for PEC water oxidation compared to pure $BiVO_4$.[6] However, these materials showed kinetic limitations for the OER, unlike PEC oxidation of sacrificial reagent (SO_3^{2-}). In this paper, we report the application of the modified SECM technique to study electrocatalysts for PEC water oxidation on semiconductor photoelectrodes. We have tested oxides of Ir, Co, Mn, Ni, NiFe, and Fe, as well as Pt metal using the SECM technique and found that Co_3O_4, Co-Pi, and Pt are effective catalysts on the BiVW-O film for PEC water oxidation.

EXPERIMENTAL SECTION

Materials. $Bi(NO_3)_3 \cdot 5H_2O$, VCl_3, $Co(NO_3)_2$ (Sigma-Aldrich), $(NH_4)_{10}W_{12}O_{41} \cdot 5H_2O$, K_2PtCl_4, $(NH_4)_2IrCl_6$ (Strem Chemicals), H_2PtCl_6, K_2IrCl_6, $IrCl_3$ (Alfa Aesar), NaH_2PO_4, Na_2HPO_4, Na_2SO_3, H_2SO_4, ethylene glycol (Fisher Scientific) were used as received. Milli-Q deionized (DI) water was used to prepare aqueous solutions for electrochemistry experiments. F-doped tin oxide (FTO) coated glass (<14 Ω, Pilkington, Toledo, OH) was used as substrate and cut into 15 mm ×15 mm pieces to prepare electrocatalyst arrays and thin films. Ir oxide nanoparticles (diameter ~2 nm) were prepared following previously described methods.[40,41]

Preparation of Electrocatalyst Arrays on BiVW-O Film. All of the BiVW-O films utilized in this paper were prepared by a drop cast method as follows. A premixed Bi, V, and W precursor solution with a molar ratio of 4.5:5:0.5 in ethylene glycol at 10 mM concentration (total of three elements) was prepared, and 100 μL of the mixed precursor solution was pipetted onto the FTO substrate (15 × 15 mm) followed by annealing with 1 °C increment per min heating to 500 °C and held at this level for 3 h in air to produce a film about 400 nm thick. Then, a pL solution dispenser (model 1550, CH Instruments, Austin, TX) was used to prepare the metal-oxide electrocatalyst arrays on the BiVW-O films. The dispenser is composed of a stepper-motor-operated XYZ stage with a piezoelectric dispensing tip (MicroJet AB-01-60, MicroFab, Plano, TX) attached to the head and a sample platform. The arrays were prepared by a previously reported procedure.[3,6] Briefly, the BiVW-O thin film on the FTO substrate was placed on the sample platform of the dispenser, and the XYZ stage moved the tip in a preprogrammed pattern, while the metal precursor solution (1 mM concentration in ethylene glycol) was dispensed dropwise by applying voltage pulses. The Ir oxide nanoparticle solution was dispensed as a water/glycerol (3/1) mixture with a 1 mM Ir precursor concentration. The first metal precursor solution was loaded and dispensed in a predesigned pattern onto the substrate, and after washing the tip the second component was loaded and dispensed, if necessary. The dispensed solution tended to spread and to form relatively large spots (around 1 mm diameter) compared to spots prepared on the bare FTO (~400 μm).[6] The prepared arrays were annealed again at 500 °C for 3 h in air (with 1 °C increment per min) to produce oxide materials except that Ir nanoparticle arrays were annealed at either 100 or 500 °C.

The Pt electrocatalyst array was prepared by photodeposition of Pt ion in aqueous solution on the BiVW-O film as previously shown for Pt on TiO_2.[42,43] Briefly, a BiVW-O film was prepared on FTO by the drop-casting method as described above and was assembled in a Teflon cell with an O-ring (exposed area: 1.0 cm^2). Then, 10 mM H_2PtCl_6 and 0.2 M methanol aqueous solution was poured into the cell. An optical fiber (400 μm, FT-400-URT, 3M, St. Paul, MN) connected to the xenon lamp (Oriel, 150 W) was placed in the cell perpendicular to and 50 μm away from the sample. Full Xe lamp irradiation was performed at open circuit. During irradiation, Pt ion was photoreduced on the BiVW-O, while methanol was photo-oxidized. This process resulted in a small spot of Pt on the BiVW-O film, which was not obvious visually but could be imaged photoelectrochemically in the SECM screening. The prepared Pt array was washed with copious DI water and dried under flowing Ar gas without disassembling the cell. Then it was used directly for the SECM screening experiment.

Screening of the Arrays. Screening of the electrocatalyst arrays was performed using an optical fiber-modified SECM setup described in previous papers.[3,6] Briefly, a 400-μm optical fiber coupled to a xenon lamp was connected to the tip holder of a CHI model 900B SECM instrument. The prepared electrocatalyst array was placed in a Teflon cell with an O-ring (exposed area: 1.0 cm^2). A Pt wire counter electrode and an Ag/AgCl reference electrode were used in 0.2 M sodium phosphate buffer (pH = 6.8). All potential values reported here are referenced to the Ag/AgCl electrode. The optical fiber was positioned perpendicular to the array surface at a 100 μm distance and scanned across the surface at 500 μm/s (normal screening experiments) or 100 μm/s (detection of product experiment with Pt-ring optical fiber). A 420-nm UV cutoff filter was used in visible light irradiation. During the scan a given potential was applied to the working electrode array by the SECM potentiostat. The measured photocurrent during the scan produced a color-coded two-dimensional image.

Pt-Ring Optical Fiber Electrode. The Pt-ring modified optical fiber was prepared using a commercial Au-coated optical fiber (Fiberguide Industries, Inc., Stirling, NJ) as described earlier.[3] The Au-coated optical fiber was sealed in a borosilicate glass tube with heating under vacuum. The sealing procedure was the same as that used in the preparation of UMEs for normal SECM experiments described in the literature.[44] The bottom view of the resulting optical fiber showed the Au-ring electrode surrounded by a glass insulator. The sizes of the Au-ring optical fiber used were as follows: inner diameter (diam) of the optical fiber, 200 μm; inner diam of the Au ring, 240 μm; outer diam of the Au ring, 275 μm; diam of the whole optical fiber including the glass insulator, 600 μm. Finally, the Au ring electrode was electrochemically plated with Pt by applying 0.1 V (vs Ag/AgCl) for 300 s in 1.0 mM K_2PtCl_4 in 0.1 M H_2SO_4 aqueous solution.

Preparation and PEC Measurements of Larger Area Films. For larger scale experiments, electrodes on FTO glass about 1.5 cm by 1.5 cm were fabricated. The BiVW-O film was prepared by drop coating with the same solutions and procedures as with the SECM array samples. Catalyst films on the BiVW-O were prepared by the drop-cast method (for the Co or Ir oxide catalyst) and photoreduction (for the Pt catalyst). For the drop-cast method, 50 μL of 1 mM Co or Ir precursor solutions were placed onto the BiVW-O films and annealed at 500 °C for 3 h in air in the same manner as in the array sample preparation. In case of Pt deposition by photoreduction, the BiVW-O film was soaked in 10 mM H_2PtCl_6 with 0.2 M methanol aqueous solution as the array sample, and light irradiation was performed on the whole film directly for 30 min using the Xe lamp without the

optical fiber. Co-Pi electrocatalyst films were prepared by PEC deposition. The BiVW-O film was exposed to the freshly made 0.05 mM or 0.5 mM $Co(NO_3)_2$ solution in 0.1 M sodium phosphate buffer (pH 6.8), and a constant potential (0.3 V vs Ag/AgCl) was applied with Xe lamp irradiation. The amount of deposited Co-Pi was controlled by the deposition time and the concentration of Co ion. Then, the resulting film was rinsed with copious DI water.

The resulting electrocatalyst films on BiVW-O were used as working electrodes with a 0.2 cm^2 geometric area exposed to electrolyte solution and light irradiation. All electrochemical experiments were carried out in a borosilicate glass cell using a three-electrode configuration with a Pt-gauze counter electrode and a Ag/AgCl reference electrode. Light irradiation was performed through the electrolyte solution using a Xe lamp with an incident light intensity of about 100 mW/cm^2. A UV cutoff filter (>420 nm) was used for visible light irradiation. The PEC water oxidation measurements were carried out in 0.2 M sodium phosphate buffer (pH 6.8) solution. A monochromator (Oriel) was used to measure incident photon to current conversion efficiencies (IPCE).

Characterization. The glancing incidence X-ray diffraction (XRD) measurements were performed with a Bruker-Norius D8 advanced diffractometer using a Cu Kα radiation source operated at 40 kV and 40 mA with an incidence angle of 1 degree. X-ray photoelectron spectroscopy (XPS) data were acquired using a Kratos Axis Ultra DLD instrument (Manchester, UK) with a monochromatic Al X-ray source.

RESULTS AND DISCUSSION

SECM Screening Study. To investigate the effect of electrocatalysts on PEC water oxidation on a BiVW-O film, Pt, Ir, and Co oxides were selected and tested, because these are known good electrocatalysts for the OER. The Ir and Co oxide arrays were prepared using the dispenser method from K_2IrCl_6 or $Co(NO_3)_2$ salt solutions on FTO followed by annealing at 500 °C, on the BiVW-O films (prepared by the drop-cast method as described in the Experimental Section). Figure 1 shows the SECM image of Ir/Co oxide electrocatalyst arrays on the BiVW-O films. There are six spots on the array having different compositions controlled by the number of drops dispensed. The numbers written under each spot indicate the number of drops of Ir and Co solution dispensed, which determines the composition of each spot. The top left spot is pure Ir oxide (IrO_x), while the bottom right spot is pure Co oxide (Co_3O_4). The photocurrent image of the Ir/Co oxide array on a BiVW-O film in 0.2 M sodium phosphate (pH 6.8) at 0.3 V vs Ag/AgCl under UV−visible (a) and visible light (b) irradiation was tested with the SECM for the PEC OER (Figure 1). Although IrO_x is known to be an excellent electrocatalyst for the OER, the IrO_x spot did not show any detectable enhancement of photocurrent over that of BiVW-O itself, but the addition of Co showed an improvement in the photocurrent, with the highest photocurrent being that of the pure Co_3O_4 spot. Notice that the background current (dark green color level in the image) is PEC water oxidation current on BiVW-O without electrocatalyst. This current can be always used as an internal standard to judge the effect of the electrocatalyst. This is one of the important advantages of using the SECM technique in this study, because one can minimize irreproducibility of the results as each sample (spot) has an internal standard for comparison. When the light source was blocked during the scan, the current on

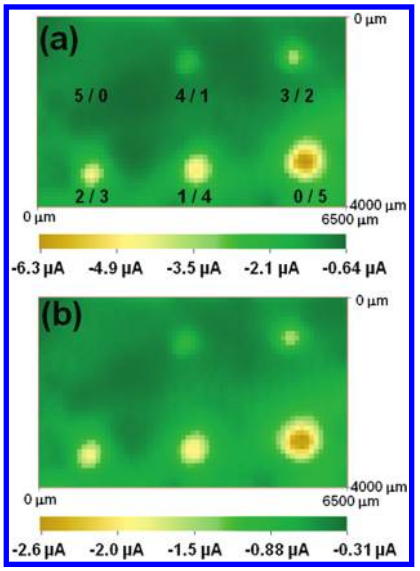

Figure 1. SECM images of Ir/Co oxide array on the BiVW-O film at 0.3 V (vs Ag/AgCl) in 0.2 M sodium phosphate buffer (pH 6.8) under (a) UV−visible and (b) visible light irradiation. Numbers under each spot represent the number of drops of dispensed Ir and Co solutions, respectively.

the spot and background dropped to the same level, about 0.2 μA, which confirmed the measured current both on BiVW-O only or with electrocatalyst being mainly from PEC water oxidation (Figure S1 in the Supporting Information). We also performed a SECM experiment using a Co/Ir on BiVW-O film array with 0.1 M Na_2SO_3 as a sacrificial electron donor in 0.2 M phosphate buffer solution (pH 6.8). The results show that there is no difference between presence and absence of any Co/Ir electrocatalyst (Figure S2 in the Supporting Information). This result confirms that the Co oxide acts as an electrocatalyst for the water oxidation reaction and not as a photoelectrode to generate electron−hole pairs.

We also prepared arrays with other Ir metal precursors ($(NH_4)_2IrCl_6$ and $IrCl_3$) as well as IrO_x nanoparticles to make IrO_x arrays on BiVW-O films, and all showed no detectable improvement in SECM screening in 0.2 M sodium phosphate at 0.3 V vs Ag/AgCl under UV−visible and visible light irradiation. We also tested other metal (Mn, Ni, NiFe, Cu) oxide electrocatalyst arrays in the same manner and none of them showed any photocurrent changes as electrocatalyst spots for PEC water oxidation in the SECM test. In other words, we could not obtain a SECM image showing any of these electrocatalyst spots above the BiVW-O background.

A Pt array was also prepared on BiVW-O film and tested using SECM, because Pt is also a well-known electrocatalyst for the OER. Here, the Pt array was fabricated by photoreduction of a K_2PtCl_4 solution as described in the Experimental Section instead of the dispensing technique used for the oxide electrocatalyst preparation. Three Pt spots were prepared with different deposition times (20, 30, and 40 min). Figure 2 shows SECM images of three Pt spots on BiVW-O film in 0.2 M phosphate buffer at 0.2 V (vs Ag/AgCl) under UV−visible (a) and visible (b) light. All three spots show relatively high photocurrents compared to background. The 30-min spot showed a higher photocurrent than the 20-min spot and was almost the same photocurrent as a 40-min spot, which means that 30 min of photodeposition time is enough to reach optimum deposition. In

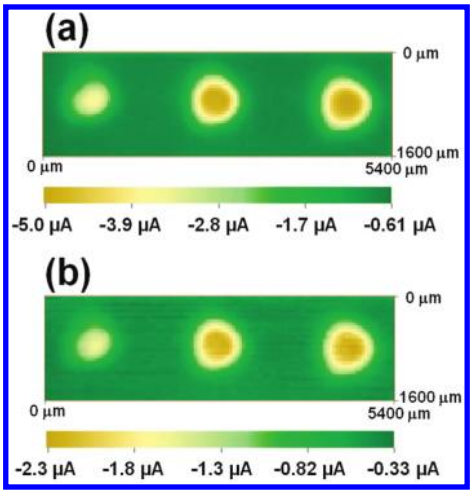

Figure 2. SECM images of Pt array on the BiVW-O film at 0.3 V in 0.2 M sodium phosphate buffer (pH 6.8) under (a) UV-visible and (b) visible light irradiation. Pt spots were fabricated by photoreduction of Pt precursor under UV−visible light irradiation through an optical fiber for 20, 30, and 40 min (left to right).

addition, a SECM experiment was performed in 0.2 M phosphate buffer (pH 6.8) with 0.1 M Na_2SO_3 as a sacrificial donor. The SECM image here shows lower photocurrent on the Pt spots (Figure S3 in the Supporting Information); the negative effect for the oxidation reaction of SO_3^{2-} is probably because of light absorption by the Pt layer.

Detection of Products. To investigate the product generated by the PEC water oxidation reaction on the electrocatalyst array on BiVW-O film, a Pt ring-optical fiber was used as described in the Experimental Section. Parts a and b of Figure 3 show SECM images of the anodic photocurrent at a Co_3O_4 spot on a BiVW-O film on the substrate (at 0.3 V) and the cathodic current at the Pt ring (at −0.2 V) in Ar-saturated 0.2 M phosphate buffer solution under UV−visible light illumination. In this experiment, water was oxidized to oxygen on the spot, and the oxygen produced was reduced on the Pt ring electrode. A higher current was observed on the Co_3O_4 spot compared to the BiVW-O background not only on the substrate image but also on the ring image. A Pt spot on a BiVW-O film exhibited similar SECM images for the substrate and ring electrode (Figure 4). These results also confirm that the photocurrent increase found with the Co_3O_4 and Pt spots are consistent with more water oxidation to O_2 on those spots than on bare BiVW-O. Note that one cannot directly compare photocurrents for the Co_3O_4 and Pt spots because the light intensity in Figures 3 and 4 is different because of variations in the alignment of the optical fiber, lamp, and array.

Bulk Film Study. To confirm that the results observed in the SECM study are applicable to large-scale films, we prepared bulk Co_3O_4 on the BiVW-O film (denoted as Co/BiVW-O) as described in the Experimental Section. The amount of deposited Co_3O_4 was about 5 mol % compared to the amount of BiVW-O used (50 μL of 1 mM Co precursor solution and 100 μL of 10 mM Bi/V/W precursor solution). We also tested different amounts of Co (0.5, 1, 10 mol %), and more Co produced higher photocurrents, except that 5 and 10 mol % Co films showed similar photocurrents. We then compared their PEC OER activity to BiVW-O only films using linear sweep voltammetry (LSV). Figure 5b shows the LSV of a Co/BiVW-O film in 0.2 M phosphate buffer solution under UV−visible and visible light irradiation and in the dark with a potential sweep from −0.1 to

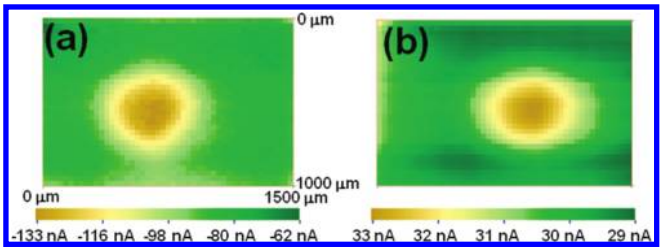

Figure 3. SECM images of (a) photocurrent at Co_3O_4 spot on the substrate at 0.3 V and (b) current at the ring at −0.2 V in Ar-saturated 0.2 M sodium phosphate buffer (pH 6.8) solution under UV−vis light irradiation. Negative current is anodic current and positive current is cathodic current.

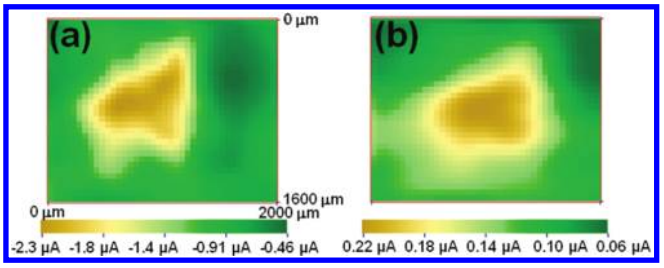

Figure 4. SECM images of (a) photocurrent at Pt spot on the substrate at 0.3 V and (b) current on the ring at −0.2 V (b) in Ar-saturated 0.2 M sodium phosphate buffer (pH 6.8) solution under UV−vis light irradiation. Negative current is anodic current and positive current is cathodic current.

0.7 V vs Ag/AgCl at a scan rate of 20 mV/s. Compared to a BiVW-O film (Figure 5a) the Co/BiVW-O film showed higher photocurrent over the whole potential range, especially in the region of less positive potentials producing a different shape for the voltammogram (showing a higher fill factor). This can be attributed to the electrocatalytic effect of Co_3O_4 on the OER. Bulk IrO_x films were also prepared on BiVW-O (Ir/BiVW-O) with different loadings of 0.2, 0.5, 1, 5, and 10 mol % relative to the total amount of Bi, V, and W. They were then tested for PEC water oxidation under the same conditions. The LSV of these films are shown in Figure S4 in the Supporting Information. Only the 0.5 and 1 mol % IrO_x films showed a little better fill factor in LSV with UV−visible light irradiation, while others showed lower photocurrents than the BiVW-O film without electrocatalysts. Moreover, the 0.5 and 1% IrO_x films suffered from an apparent instability and photocurrents decreased strongly with the number of LSV scans and eventually exhibited lower currents than those of the BiVW-O only film, especially in the high overpotential region. In contrast, Co/BiVW-O and those with two electrocatalysts on BiVW-O films (Pt/BiVW-O and Co-Pi/BiVW-O) discussed below showed stable photocurrents. Over 80% of initial photocurrents were observed in the CV scans or at a constant potential of 0.2 V (vs Ag/AgCl) for at least 1 h.

We also prepared a large Pt electrode on BiVW-O film (Pt/BiVW-O) by photodeposition. Figure 5c shows the LSV of Pt/BiVW-O, and the result is quite similar to the Co_3O_4 case, with an even higher photocurrent. Figure 6 shows a comparison of the LSV of the three samples in Figure 5 by chopping the light every 5 s (light on and 2.5 s light off) under UV−visible light irradiation. The results show comparable photocurrent to the LSV shown in Figure 5 and instantaneous current response with the light on and off response typical for a PEC effect.

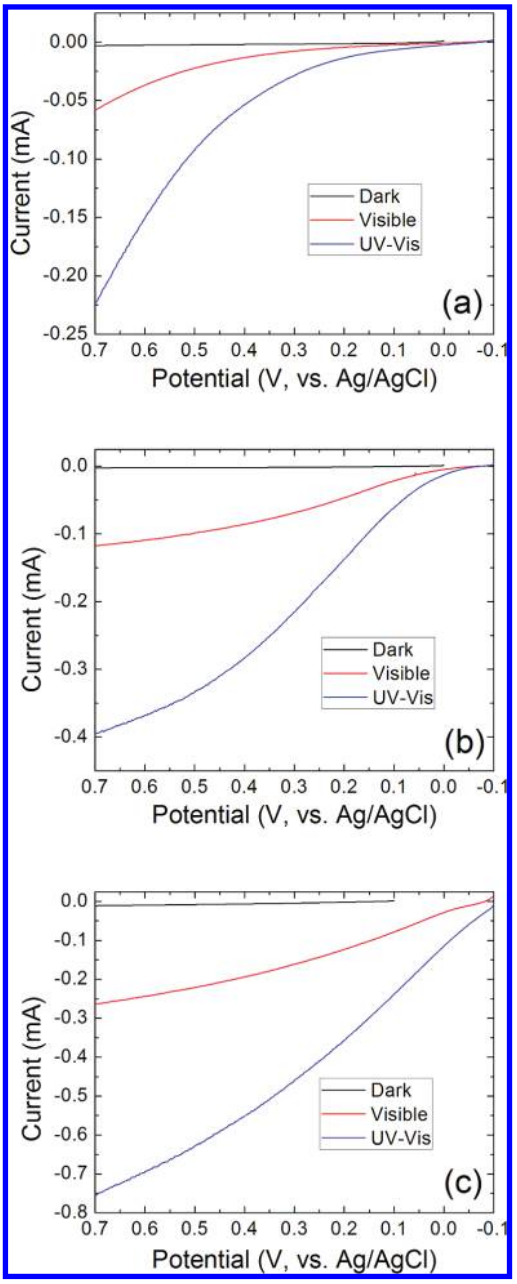

Figure 5. LSVs of (a) BiVW-O only, (b) Co/BiVW-O, and (c) Pt/BiVW-O films in 0.2 M sodium phosphate buffer (pH 6.8) under dark, visible, and UV−visible irradiation. Scan rate: 20 mV/s. Electrode area: 0.2 cm^2.

A variation of the cobalt oxide electrode catalyst, represented as Co-Pi, prepared by electrodeposition has recently been proposed as an electrocatalyst for the OER.[29−31] We thus prepared Co-Pi arrays on a BiVW-O film by photo-oxidation of a Co solution with light irradiation through an optical fiber similar to array preparation with Pt on a BiVW-O film and tested these using the SECM technique. However, it was difficult to see any spots in the array image because the BiVW-O film area, which was not irradiated but had been contacted by the Co^{2+} solution, showed a photocurrent improvement. Co^{2+} treatment of hematite has been shown to improve for the PEC OER.[35] Thus, Co-Pi was studied only with larger films. The Co-Pi electrocatalyst film was prepared on BiVW-O films by photo-oxidation of $Co(NO_3)_2$

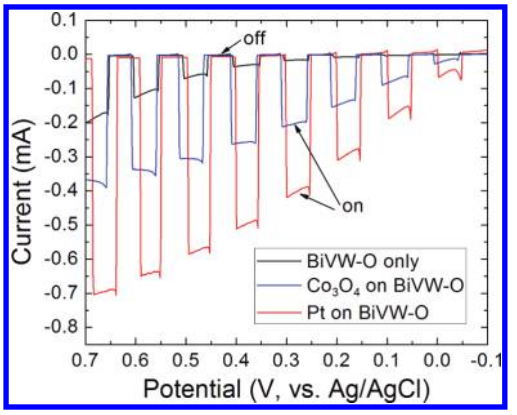

Figure 6. LSVs of BiVW-O only, Co/BiVW-O, and Pt/BiVW-O films with light chopping in 0.2 M sodium phosphate buffer (pH 6.8) under UV−visible light irradiation. Scan rate: 20 mV/s. Electrode area: 0.2 cm^2.

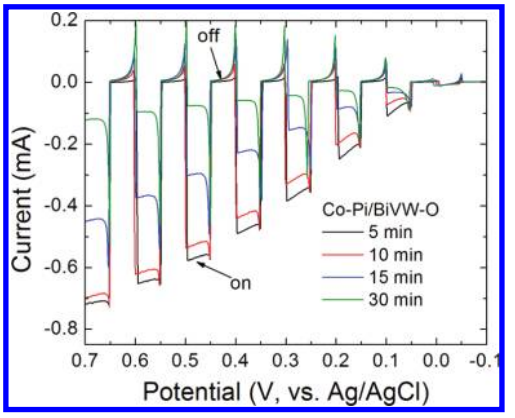

Figure 7. LSVs of Co-Pi/BiVW-O films with various Co-Pi deposition times (5, 10, 15, and 30 min) in 0.2 M sodium phosphate buffer (pH 6.8) under UV−visible light irradiation. Scan rate: 20 mV/s. The concentration of $Co(NO_3)_2$ in Co-Pi deposition process was 0.05 mM. Electrode area: 0.2 cm^2.

in phosphate buffer as described in the Experimental Section. Figure 7 shows LSV of Co-Pi covered BiVW-O films (Co-Pi/BiVW-O) in a 0.2 M phosphate buffer solution under UV−visible light irradiation. The Co-Pi/BiVW-O films with 5 min Co-Pi deposition showed the highest photocurrent, which decreased with longer deposition times. There were also larger current transients on both the light-on and light-off points with longer Co-Pi depositions, suggesting more recombination processes. Note that the concentration of $Co(NO_3)_2$ in the Co-Pi deposition solution was only 0.05 mM. When Co-Pi was deposited at a 0.5 mM concentration of $Co(NO_3)_2$, there was only a small photocurrent and large current transients even with a 30 s or 5 min deposition of Co-Pi on BiVW-O (see Figure S5 in the Supporting Information).

The films were also tested for longer time stability. With Pt, after a small decay, the current was then stable for at least 6 h. However for the IrO_2 film, there was a continuous decay to levels even lower than the uncatalyzed film (see Figure S4 in the Supporting Information).

Incident Photon to Current Conversion Efficiency (IPCE) Measurements. IPCE measurements of Co_3O_4, Pt, Co-Pi-coated BiVW-O films, as well as uncoated BiVW-O were carried

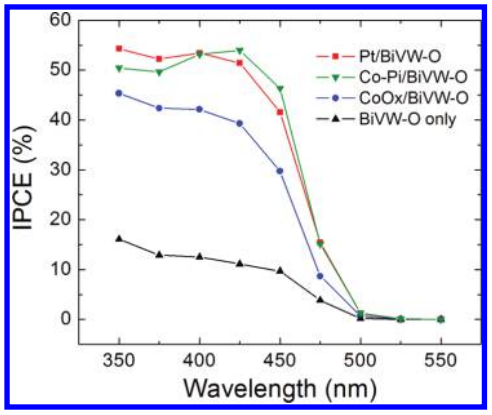

Figure 8. IPCE plots of Pt/BiVW-O, Co-Pi/BiVW-O, Co/BiVW-O, and BiVW-O calculated from the photocurrents at 0.63 V vs Ag/AgCl.

out at 0.63 V vs Ag/AgCl (the thermodynamic potential of water oxidation at pH 6.8) under monochromatic light irradiation. Figure 8 shows IPCE plots of three films over the range 350−550 nm calculated with the following equation

$$\mathrm{IPCE}(\%) = 1240 \times (i_{\mathrm{ph}}/\lambda P_{\mathrm{in}}) \times 100 \qquad (1)$$

where i_{ph} is the photocurrent (mA), λ the wavelength (nm) of incident radiation, and P_{in} the incident light power intensity on the semiconductor electrode (mW). The Pt/BiVW-O and Co-Pi/BiVW-O films showed high IPCE values reaching up to 55% at λ < 450 nm with the Co/BiVW-O film ~45% in the same region; the BiVW-O film without electrocatalyst showed only ~15%. The IPCE values decreased with increasing wavelength and were almost zero at 500 nm (2.5 eV) for all films, suggesting no difference in the band gap energy of these films. In fact, the IPCE values of the Pt/BiVW-O and Co-Pi films are similar to those found earlier for an unmodified BiVW-O film for the PEC oxidation of a sacrificial agent (SO_3^{2-}).[6]

Comparison to Dark OER on Electrocatalyst Films on FTO. Electrocatalyst films were prepared directly on bare FTO, and their electrocatalytic behavior was tested for the dark OER using LSV. Co_3O_4 and IrO_x films were prepared in exactly the same way as in the large film studies on BiVW-O except that bare FTO was used as the substrate and the electrocatalyst amount was increased about 10 times. The Co-Pi film was prepared on bare FTO by applying 1.1 V (vs Ag/AgCl) in 0.5 mM $Co(NO_3)_2$ and 0.1 M sodium phosphate buffer solution for 10 min. A Pt disk electrode was used to compare Pt behavior, and the electrode area was normalized against the area used for other catalyst films. Figure 9 shows cyclic voltammograms of Co_3O_4, Co-Pi, IrO_x films, Pt disk, and bare FTO electrodes in 0.2 M phosphate buffer (pH 6.8). IrO_x showed the highest activity for water oxidation, while Co-Pi, Co_3O_4, and Pt follows, respectively. This order of activity is opposite to that obtained with BiVW-O oxide films.

This difference in dark electrocatalytic activity and that on a photocatalyst surface is surprising but can be ascribed to several sources. If the film of the catalyst, e.g., IrO_2, is sufficiently thick to absorb appreciable amounts of incident radiation, it will clearly decrease the production of carriers in the photocatalyst and decrease the current. For the studies here, measurements of absorptivity suggest that this is not a significant source of the decrease in activity with BiVW-O (See Figure S6 in the Supporting Information). Another factor is the nature of the electrocatalyst/photocatalyst junction. For example, poor contact at the

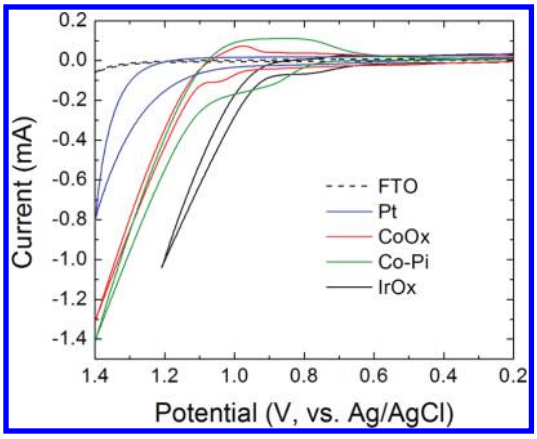

Figure 9. Cyclic voltammograms of bare FTO, Co_3O_4, Co-Pi, IrO_x, and Pt in 0.2 M sodium phosphate buffer (pH 6.8). Scan rate: 50 mV/s. CV of Pt was obtained on a commercial Pt disk electrode (diameter = 2 mm) and normalized by the area (0.2 cm^2) of other electrodes for comparison.

interface could cause ohmic losses, and the junction might also increase recombination at the interface. In considering the effect of contact or interactions between electrocatalyst and photocatalyst, i.e., IrO_2 and BiVW-O, several different methods of making IrO_x on photocatalyst films were tried, e.g., by attaching IrO_x nanoparticles or casting and annealing various Ir precursors, e.g., K_2IrCl_6, $(NH_4)_2IrCl_6$, and $IrCl_3$, on the BiVW-O film. However, the IrO_x prepared from various sources did not show significant differences on BiVW-O. Possibly adsorbate−electrocatalyst or adsorbate−photocatalyst interactions including electrocatalyst−photocatalyst interactions have significant effects on the OER activity of the electrocatalysts. However, a detailed study on these interfacial interactions is beyond the scope of this paper, and the generality of these findings remains to be explored.

Characterization. The Bi/V/W oxide material was characterized by XRD and XPS. An XPS experiment on Co/BiVW-O and Pt/BiVW-O was also performed to verify the oxidation state of Co and Pt before and after the PEC OER experiment. The Co peak position matched well for the peak of Co_3O_4 in the literature.[45] However, the Pt electrocatalysts mainly showed PtO_2 at 74.8 eV with a small peak at 72.5 eV corresponding to zerovalent Pt. The zerovalent peak disappeared after additional PEC water oxidation experiments. This result suggests that the surface of the Pt electrocatalyst film prepared by photodeposition is mainly PtO_2 after OER experiments (Figure S7 in the Supporting Information). However, since XPS can only analyze the surface of the film (several nanometers), this probably represents a surface layer on zerovalent Pt.

XRD experiments were also carried out for a film of Co_3O_4 alone on a glass substrate using larger amounts of catalyst prepared in the same way as the spots, because the Co_3O_4 film of Co/BiVW-O was too thin to get an XRD signal. The resulting pattern agreed well with the reference pattern of Co_3O_4 (Figure S8 in the Supporting Information), confirming that the film produced by drop coating with a $Co(NO_3)_2$ solution followed by heating in air at 500 °C, produces this material.

CONCLUSIONS

We have demonstrated that the optical fiber-modified SECM technique can be used to quickly identify the effect of various electrocatalysts for PEC OER (water oxidation) on semiconductor

photoelectrodes. Pt and Co_3O_4 were found to be effective electrocatalysts on BiVW-O films, while IrO_x was not active, even though IrO_x films showed the highest electrocatalytic activity for water oxidation as a dark electrocatalyst. The optical fiber modified with a Pt ring electrode was utilized to electrochemically detect the product (O_2) of the PEC reaction on Co_3O_4 and Pt coated BiVW-O. These SECM results were confirmed with linear sweep voltammetry using PEC with larger electrodes with the same films. Furthermore, Co-Pi electrocatalyst was also tested on a BiVW-O film with a larger electrode for PEC water oxidation and showed similar photocurrent enhancement as Pt and Co_3O_4.

The SECM method can be used to optimize electrocatalysts rapidly, e.g., by investigating different compositions with mixed electrocatalysts and by changing their thickness by dispensing blank solutions or with changing concentration of precursor solutions.

■ ASSOCIATED CONTENT

Supporting Information. Additional experimental data figures. This material is available free of charge via the Internet at http://pubs.acs.org

■ AUTHOR INFORMATION

Corresponding Author
*E-mail: ajbard@mail.utexas.edu.

■ ACKNOWLEDGMENT

We appreciate the National Science Foundation (CHE-0934450) for financial support of this project. We thank the National Science Foundation (Grant No. 0618242) for funding the purchase of the X-ray photoelectron spectrometer used in this work. We also thank Dr. Seong Jung Kwon for the synthesis of the IrO_x nanoparticles.

■ REFERENCES

(1) Fernandez, J. L.; Walsh, D. A.; Bard, A. J. *J. Am. Chem. Soc.* **2005**, *127*, 357.
(2) Minguzzi, A.; Alpuche-Aviles, M. A.; Rodríguez López, J.; Rondinini, S.; Bard, A. J. *Anal. Chem.* **2008**, *80*, 4055.
(3) Lee, J.; Ye, H.; Pan, S.; Bard, A. J. *Anal. Chem.* **2008**, *80*, 7445.
(4) Jang, J. S.; Lee, J.; Ye, H.; Fan, F.-R. F.; Bard, A. J. *J. Phys. Chem. C* **2009**, *113*, 6719.
(5) Liu, W.; Ye, H.; Bard, A. J. *J. Phys. Chem. C* **2010**, *114*, 1201.
(6) Ye, H.; Lee, J.; Jang, J. S.; Bard, A. J. *J. Phys. Chem. C* **2010**, *114*, 13322.
(7) Fujishima, A.; Honda, K. *Nature* **1972**, *238*, 37.
(8) Harriman, A.; Pickering, I. J.; Thomas, J. M.; Christensen, P. A. *J. Chem. Soc., Faraday Trans.* **1988**, *84*, 2795.
(9) Hara, M.; Waraksa, C. C.; Lean, J. T.; Lewis, B. A.; Mallouk, T. E. *J. Phys. Chem. A* **2000**, *104*, 5275.
(10) Morris, N. D.; Suzuki, M.; Mallouk, T. E. *J. Phys. Chem. A* **2004**, *108*, 9115.
(11) Jiao, F.; Frei, H. *Angew. Chem., Int. Ed.* **2009**, *48*, 1841.
(12) Jiao, F.; Frei, H. *Chem. Commun.* **2010**, *46*, 2920.
(13) Ishikawa, A.; Takata, T.; Kondo, J. N.; Hara, M.; Kobayahi, H.; Domen, K. *J. Am. Chem. Soc.* **2002**, *124*, 13547.
(14) Iwase, A.; Kato, H.; Kudo, A. *Chem. Lett.* **2005**, *34*, 946.
(15) Maeda, K.; Xiong, A.; Yoshinaga, T.; Ikeda, T.; Sakamoto, N.; Hisatomi, T.; Takashima, M.; Lu, D.; Kanehara, M.; Setoyama, T.; Teranishi, T.; Domen, K. *Chem. Commun.* **2010**, *49*, 4096.
(16) Yagi, M.; Tomita, E.; Sakita, S.; Kuwabara, T.; Nagai, K. *J. Phys. Chem. B* **2005**, *109*, 21489.
(17) Kuwabara, T.; Tomita, E.; Sakita, S.; Hasegawa, D.; Sone, K.; Yagi, M. *J. Phys. Chem. C* **2008**, *112*, 3774.
(18) Nakagawa, T.; Beasley, C. A.; Murray, R. W. *J. Phys. Chem. C* **2009**, *113*, 12958.
(19) Kiwi, J.; Grätzel, M. *Angew. Chem., Int. Ed.* **1978**, *17*, 860.
(20) Kibria, M. F.; Mridha, M. Sh. *Int. J. Hydrogen Energy* **1996**, *21*, 179.
(21) Miller, E. L.; Rocheleau, R. E. *J. Electrochem. Soc.* **1997**, *144*, 1995.
(22) Corrigan, D. A. *J. Electrochem. Soc.* **1987**, *134*, 377.
(23) Miller, E.; Rocheleau, R. E. *J. Electrochem. Soc.* **1997**, *144*, 3072.
(24) Merrill, M. D.; Dougherty, R. C. *J. Phys. Chem. C* **2008**, *112*, 3655.
(25) Iwakura, C.; Honji, A.; Tamura, H. *Electrochim. Acta* **1981**, *26*, 1319.
(26) Rasiyah, P.; Tseung, A. C. C. *J. Electrochem. Soc.* **1983**, *130*, 365.
(27) Singh, R. N.; Mishra, D.; Anindita; Sinha, A. S. K.; Singh, A. *Electrochem. Commun.* **2007**, *9*, 1369.
(28) Esswein, A. J.; McMurdo, M. J.; Ross, P. N.; Bell, A. T.; Tilley, T. D. *J. Phys. Chem. C* **2009**, *113*, 15068.
(29) Kanan, M. W.; Nocera, D. G. *Science* **2008**, *321*, 1072.
(30) Surendranath, Y.; Dincă, M.; Nocera, D. G. *J. Am. Chem. Soc.* **2009**, *131*, 2615.
(31) Lutterman, D. A.; Surendranath, Y.; Nocera, D. G. *J. Am. Chem. Soc.* **2009**, *131*, 3838.
(32) Dincă, M.; Surendranath, Y.; Nocera, D. G. *Proc. Natl. Acad. Sci.* **2010**, *107*, 10337.
(33) Trasatti, S.; Lodi, G. Oxygen and Chlorine Evolution at Conductive Metallic Oxide Anodes. In *Electrodes of Conductive Metallic Oxides Part B*; Trasatti, S., Ed.; Studies in Physical and Theoretical Chemistry Series 11B; Elsevier Scientific: Amsterdam, The Netherlands, 1981; pp 521−626.
(34) Matsumoto, Y.; Sato, E. *Mater. Chem. Phys.* **1986**, *14*, 397.
(35) Kay, A.; Cesar, I.; Grätzel, M. *J. Am. Chem. Soc.* **2006**, *128*, 15714.
(36) Tilley, S. D.; Cornuz, M.; Sivula, K.; Grätzel, M. *Angew. Chem., Int. Ed.* **2010**, *49*, 1.
(37) Zhong, D. K.; Sun, J.; Inumaru, H.; Gamelin, D. R. *J. Am. Chem. Soc.* **2009**, *131*, 6086.
(38) Zhong, D. K.; Gamelin, D. R. *J. Am. Chem. Soc.* **2010**, *132*, 4202.
(39) Kleiman-Shwarsctein, A.; Hu, Y.-S.; Stucky, G. D.; McFarland, E. W. *Electrochem. Commun.* **2009**, *11*, 1150.
(40) Nakagawa, T.; Bjorge, N. S.; Murray, R. W. *J. Am. Chem. Soc.* **2009**, *131*, 15578.
(41) Kwon, S. J.; Fan, F.-R. F.; Bard, A. J. *J. Am. Chem. Soc.* **2010**, *132*, 13165.
(42) Kraeutler, B.; Bard, A. J. *J. Am. Chem. Soc.* **1978**, *100*, 4317.
(43) Yang, J. C.; Kim, Y. C.; Shul, Y. G.; Shin, C. H.; Lee, T. K. *Appl. Surf. Sci.* **1997**, *121−122*, 525.
(44) *Scanning Electrochemical Microscopy*; Bard, A. J., Mirkin, M. V., Eds.; Marcel Dekker: New York, 2001.
(45) NIST X-ray Photoelectron Spectroscopy Database, NIST Standard Reference Database 20, Version 3.5. http://srdata.nist.gov/xps/ (accessed August, 2010).